SCIENCE CHINA
Earth Sciences

• RESEARCH PAPER •

March 2013 Vol.56 No.3: 434–443
doi: 10.1007/s11430-012-4568-z

The role of constant optimal forcing in correcting forecast models

FENG Fan[1,2] & DUAN WanSuo[1*]

[1] *LASG, Institute of Atmospheric Physics, Chinese Academy of Sciences, Beijing 100029, China;*
[2] *University of Chinese Academy of Sciences, Beijing 100049, China*

Received April 13, 2012; accepted August 7, 2012; published online January 16, 2013

In this paper, the role of constant optimal forcing (COF) in correcting forecast models was numerically studied using the well-known Lorenz 63 model. The results show that when we only consider model error caused by parameter error, which also changes with the development of state variables in a numerical model, the impact of such model error on forecast uncertainties can be offset by superimposing COF on the tendency equations in the numerical model. The COF can also offset the impact of model error caused by stochastic processes. In reality, the forecast results of numerical models are simultaneously influenced by parameter uncertainty and stochastic process as well as their interactions. Our results indicate that COF is also able to significantly offset the impact of such hybrid model error on forecast results. In summary, although the variation in the model error due to physical process is time-dependent, the superimposition of COF on the numerical model is an effective approach to reducing the influence of model error on forecast results. Therefore, the COF method may be an effective approach to correcting numerical models and thus improving the forecast capability of models.

predictability, prediction error, model error, optimal forcing

Citation: Feng F, Duan W S. The role of constant optimal forcing in correcting forecast models. Science China: Earth Sciences, 2013, 56: 434–443, doi: 10.1007/s11430-012-4568-z

The study of the uncertainty of the forecast results (prediction error) is a core of predictability studies on numerical weather forecasting and climate prediction. The uncertainty is usually caused by both initial and model errors. To study the role of initial and model errors independently, Lorenz [1] divided the predictability problem into two types. The first type of predictability problem mainly concerns the uncertainty of the forecast results caused by initial error, whereas the second type of predictability problem addresses the uncertainty generated by model error. Due to the development of nonlinear theory [2, 3], meteorological data, and numerical models [4, 5], the impact of initial error on predictability has been extensively studied [6–10]. Several methods associated with the first type of predictability have been proposed, such as the conditional nonlinear optimal perturbation (CNOP) method [11], the four-dimensional variational data assimilation method [12], and the Ensemble Kalman Filter [13] method. All these methods are effective for correcting the initial fields to overcome the uncertainty of the initial condition. A common feature of these studies is that the forecast models are assumed to be perfect without any model error; therefore, the prediction errors are derived solely from the initial errors. However, in realistic cases, the model equations and the control parameters cannot be given exactly, thus resulting in the inevitable effect of model error on the forecast result. Therefore, it is important to study and subsequently control model errors.

The atmosphere, oceans, land surface and their coupled systems are typical nonlinear systems, and their characteristics determine that there is an upper limit of predictability for each of these systems. Meteorologists are seeking ways to minimize the model error to achieve the limit of the pre-

*Corresponding author (email: duanws@lasg.iap.ac.cn)

dictability. Efforts to reduce model error have been made by improving model resolution, parameterizing physical processes, offsetting model errors by external forcing, and using computer technology with greater accuracy. Ren et al. [14] commented on these methods and identified the advantages and disadvantages of them, thereby providing guidance for the further application of the above methods.

D'Andrea and Vautard [15] suggested that if observations for a certain time interval are known, one can superimpose an appropriate constant forcing associated with these observations to the tendency equations and correct the model closest to the observations, thereby generating a modified model with forcing for improved forecast results. Roads [16] and Vannitsem and Toth [17] also used a similar approach to reducing the effects of model error. If only time-invariant system errors exist in the models, it is then conceivable that model error can be offset by superposing a proper constant forcing on the numerical model. However, model error usually includes both the time-invariant system error and other types of time-varying model error. Therefore, in the case where the model error varies with time, the question of whether the constant forcing remains an effective approach to offsetting model error and improving the forecast capability is not known. This is the main issue that we will discuss later in this paper.

1 Constant optimal forcing

Consider a nonlinear partial differential equation(s):

$$\begin{cases} \dfrac{\partial \mathbf{u}}{\partial t} = F(\mathbf{u}, t), \\ \mathbf{u}\big|_{t=0} = \mathbf{u}_0, \end{cases} \tag{1.1}$$

where $\mathbf{u}(\mathbf{x},t) = [u_1(\mathbf{x},t),\ u_2(\mathbf{x},t),\ ...,\ u_n(\mathbf{x},t)]$ is the state vector, F is a nonlinear operator, $\mathbf{u}_0$ is the initial state, $(\mathbf{x},t) \in \Omega \times [0,T]$, Ω is a domain in R^n, $T < +\infty$, $\mathbf{x} = (x_1, x_2, ..., x_n)$, and t is the time. Suppose we use the model described by eqs. (1.1) to predict the motion of the atmosphere or oceans, but the model is associated with model errors. For the given initial field $\mathbf{u}_0$, the solution to eqs. (1.1) for the state vector $\mathbf{u}$ at time τ is given by

$$\mathbf{u}(\mathbf{x}, \tau) = M_\tau(\mathbf{u}_0). \tag{1.2}$$

Here, M_τ is the propagator.

If the initial field is exact, then the prediction error caused by model error can be defined as

$$E_\tau = \left\| M_\tau(\mathbf{u}_0^r) - \mathbf{u}_\tau^r \right\|, \tag{1.3}$$

where $\mathbf{u}_0^r$ is the true state at the initial time, $\mathbf{u}_\tau^r$ is the true state at time τ, and $\|\cdot\|$ is a given norm used to measure the magnitudes of the prediction errors. The true states of the atmosphere and ocean motions cannot be known exactly; therefore, in this paper, we take observations to be sufficiently accurate approximations of the true state $\mathbf{u}_\tau^r$ [18]. Let the observations at time 0 and τ be $\mathbf{u}_0^{\text{obs}}$ and $\mathbf{u}_\tau^{\text{obs}}$ respectively; then, the prediction error caused by model error can be approximately written as

$$E_\tau = \left\| M_\tau(\mathbf{u}_0^{obs}) - \mathbf{u}_\tau^{obs} \right\|. \tag{1.4}$$

In the following text, we discuss the model error based on eq. (1.4).

For a given time T, let the observations at time T and initial time be $\mathbf{u}_T^{\text{obs}}$ and $\mathbf{u}_0^{\text{obs}}$, respectively. The prediction error caused by model error of eqs. (1.1) is E_T. As mentioned in the introduction, D'Andrea and Vautard [15] reduced the model error by adding a constant forcing (also known as model perturbation) $\mathbf{f}(\mathbf{x})$ to the original model:

$$\begin{cases} \dfrac{\partial \mathbf{u}}{\partial t} = F(\mathbf{u}, t) + \mathbf{f}(\mathbf{x}), \\ \mathbf{u}\big|_{t=0} = \mathbf{u}_0. \end{cases} \tag{1.5}$$

Considering this approach, we pose the following question: how can an external forcing $\mathbf{f}(\mathbf{x})$ be "the most effective" in correcting the model? To address this question, we can turn the above problem into a type of nonlinear optimization problem [15, 17]. That is, the optimization problem can consider that certain $\mathbf{f}(\mathbf{x})$ is chosen such that the difference between the model predictions and the observations is minimized. Suppose M_T^f is the discrete propagator of eqs. (1.5) from 0 to time T; then, the following unconstrained optimization problem can be solved:

$$J(\mathbf{f}^*) = \min_{\mathbf{f}} J(\mathbf{f}), \tag{1.6}$$

where

$$J(\mathbf{f}) = \left\| M_T^{\mathbf{f}}(\mathbf{u}_0^{\text{obs}})(\mathbf{f}) - \mathbf{u}_T^{\text{obs}} \right\|. \tag{1.7}$$

The obtained $\mathbf{f}^*$ is the model perturbation that produces model forecast results closest to the observation at the prediction time T; this model perturbation is called "constant optimal forcing" (COF) in this paper. We can also define other types of objective functions. For example, to investigate the forecast capability of a model with respect to the variable trends in weather or climate events, we can define the objective function as minimizing the difference between the model predictions and the observations at several chosen time points within a certain time interval. In summary, the objective function associated with COF should be defined according to the physical problems of investigation.

Based on the definition of the COF, we can determine that the prediction error of the corrected model with a COF does not exceed that of the original model within the optimization time interval [0, *T*]. However, a numerical model is generally used to forecast an unknown future state, i.e., to forecast the state beyond the optimization time interval. In this case, it is necessary to determine the extent to which the COF approach improves the forecast capability. In addition, the model error (denoted by **R**) of a numerical model often changes with time, while the model perturbation used to offset model error (i.e., the COFs) is time-invariant. Naturally, we seek to determine whether the COF approach can eliminate the time-varying model error and to determine the extent to which the COF can reduce the time-varying model error. In the follow discussion, we will use the Lorenz 63 model to explore these issues.

From the above discussion, it is known that for a given norm, eqs. (1.6) and (1.7) define an unconstrained optimization problem, with the COF $\mathbf{f}^*$ being the minimum point of the objective function in the phase space. The COF can be computed via the Limited memory Broyden-Fletcher-Goldfarb-Shanno (L-BFGS) algorithm [19]. This solver adopts the gradient-steepest descent method and finds the minimum value of an objective function, in which one needs to calculate the gradient of the objective function with respect to the model perturbation. It is known that the gradient of an objective function with respect to initial perturbations is often obtained by the adjoint of the corresponding model [20]. Then can we use the adjoint to obtain the gradient of the objective function with respect to external forcing? In the next section we will address this question.

2 Computation of the constant optimal forcing

The COF is related to an unconstrained optimization problem. In a large-scale optimization, the gradient of the objective function with respect to the initial perturbations is often obtained by the adjoint method [20]. Many studies have used the adjoint method to compute the gradient of the objective function with respect to the initial perturbations, and a large number of adjoint models have been built, including the adjoint model of the two-dimensional quasi-geostrophic model, the Zebiak-Cane model [21], the MM5 model, and the WRF model, etc. The COF can also be solved using an adjoint method. Nevertheless, it should be noted that the computation of the COF requires the gradient of the objective function with respect to external forcing or model perturbation **f**. In fact, the gradient of the objective function with respect to model perturbation **f** can be transferred to a particular case of the objective function with respect to augmented initial perturbations. Next, we describe the computation of the COF using the adjoint method.

For convenience, we define the function

$$J_1(\mathbf{f}) = \frac{1}{2}\left\| M_T^f(\mathbf{u}_0^{\text{obs}})(\mathbf{f}) - \mathbf{u}_T^{\text{obs}} \right\|^2, \tag{2.1}$$

and rewrite it in the inner product form

$$J_1(\mathbf{f}) = \frac{1}{2} < \mathbf{u}'(\tau), \mathbf{u}'(\tau) >, \tag{2.2}$$

where $\mathbf{u}'(\tau)$ is the departure from the reference state (the observations) caused by model perturbation **f** and $< \bullet >$ is the inner product. The COF defined by the eqs. (1.6) and (1.7) can then be obtained by computing the minimum of $J_1(\mathbf{f})$.

The first-order variational of $J_1(\mathbf{f})$ is as follows:

$$\delta J_1 = < \mathbf{u}'(\tau), \delta\mathbf{u}'(\tau) > = \left\langle \frac{\partial J_1}{\partial \mathbf{f}}, \delta\mathbf{f} \right\rangle. \tag{2.3}$$

Furthermore, $\delta\mathbf{f}$ can be governed by the following tangent linear model:

$$\begin{cases} \dfrac{\partial \delta\mathbf{u}'}{\delta t} = \dfrac{\partial F(\mathbf{u})}{\partial \mathbf{u}}\delta\mathbf{u}' + \delta f(\mathbf{x}), \\ \dfrac{\partial \delta \boldsymbol{f}}{\partial t} = 0, \\ \delta\mathbf{u}'\big|_{t=0} = \delta\mathbf{u}'(0) = 0, \\ \delta f\big|_{t=0} = \delta\mathbf{f}(\mathbf{x}). \end{cases} \tag{2.4}$$

By introducing two Lagrangian multipliers, λ_1 and λ_2, we obtain

$$\begin{aligned} \delta J_1 =& < \mathbf{u}'(\tau), \delta\mathbf{u}'(\tau) > \\ & - \int_0^\tau \left\langle \lambda_1(t), \frac{\partial \delta\mathbf{u}'}{\delta t} - \frac{\partial F(\mathbf{u})}{\partial \mathbf{u}}\delta\mathbf{u}' - \delta \boldsymbol{f} \right\rangle \mathrm{d}t \\ & - \int_0^\tau < \lambda_2(t), \frac{\partial \delta \boldsymbol{f}}{\partial t} > \mathrm{d}t. \end{aligned} \tag{2.5}$$

Using integration by parts, we obtain

$$\begin{aligned} \int_0^\tau < \lambda_1(t), \frac{\partial \delta\mathbf{u}'}{\delta t} > \mathrm{d}t &= \int_0^\tau \frac{\partial}{\partial t} < \lambda_1(t), \delta\mathbf{u}' > \mathrm{d}t \\ & - \int_0^\tau \left\langle \frac{\partial \lambda_1(t)}{\partial t}, \delta\mathbf{u}' \right\rangle \mathrm{d}t \\ &= < \lambda_1(\tau), \delta\mathbf{u}'(\tau) > - < \lambda_1(0), \delta\mathbf{u}'(0) > \\ & - \int_0^\tau \left\langle \frac{\partial \lambda_1(t)}{\partial t}, \delta\mathbf{u}' \right\rangle \mathrm{d}t \\ &= < \lambda_1(\tau), \delta\mathbf{u}'(\tau) > - \int_0^\tau \left\langle \frac{\partial \lambda_1(t)}{\partial t}, \delta\mathbf{u}' \right\rangle \mathrm{d}t. \end{aligned}$$

$$\begin{aligned} \int_0^\tau \left\langle \lambda_2(t), \frac{\partial \delta \boldsymbol{f}}{\partial t} \right\rangle \mathrm{d}t &= \int_0^\tau \frac{\partial}{\partial t} < \lambda_2(t), \delta \boldsymbol{f} > \mathrm{d}t \\ & - \int_0^\tau \left\langle \frac{\partial \lambda_2(t)}{\partial t}, \delta \boldsymbol{f} \right\rangle \mathrm{d}t \end{aligned}$$

$$
\begin{aligned}
&=<\lambda_2(\tau),\delta\mathbf{f}(\tau)>-<\lambda_2(0),\delta\mathbf{f}(0)>\\
&-\int_0^\tau\left\langle\frac{\partial\lambda_2(t)}{\partial t},\delta\boldsymbol{f}\right\rangle\mathrm{d}t\\
&=<\lambda_2(\tau),\delta\boldsymbol{f}>-<\lambda_2(0),\delta\boldsymbol{f}>\\
&-\int_0^\tau\left\langle\frac{\partial\lambda_2(t)}{\partial t},\delta\boldsymbol{f}\right\rangle\mathrm{d}t.
\end{aligned}
$$

We then derive δJ_1 as follows:

$$
\begin{aligned}
\delta J_1 &=\int_0^\tau\left\langle\frac{\partial\lambda_1(t)}{\partial t},\delta\mathbf{u}'\right\rangle\mathrm{d}t+<\mathbf{u}'(\tau)-\lambda_1(\tau),\delta\mathbf{u}'(\tau)>\\
&+\int_0^\tau\left\langle\lambda_1(t),\left[\frac{\partial F(\mathbf{u})}{\partial\mathbf{u}}\right]\delta\mathbf{u}'\right\rangle\mathrm{d}t+\int_0^\tau<\lambda_1(t),\delta\boldsymbol{f}>\mathrm{d}t\\
&+\int_0^\tau\left\langle\frac{\partial\lambda_2(t)}{\partial t},\delta\boldsymbol{f}\right\rangle\mathrm{d}t+<0-\lambda_2(\tau),\delta\mathbf{f}>+<\lambda_2(0),\delta\mathbf{f}>\\
&=\int_0^\tau\left\langle\frac{\partial\lambda_1(t)}{\partial t},\delta\mathbf{u}'\right\rangle\mathrm{d}t+<\mathbf{u}'(\tau)-\lambda_1(\tau),\delta\mathbf{u}'(\tau)>\\
&+\int_0^\tau\left\langle\left[\frac{\partial F(\mathbf{u})}{\partial\mathbf{u}}\right]^*\lambda_1(t),\delta\mathbf{u}'\right\rangle\mathrm{d}t\\
&+\int_0^\tau<\lambda_1(t),\delta\boldsymbol{f}>\mathrm{d}t+\int_0^\tau\left\langle\frac{\partial\lambda_2(t)}{\partial t},\delta\boldsymbol{f}\right\rangle\mathrm{d}t\\
&+<0-\lambda_2(\tau),\delta\mathbf{f}>+<\lambda_2(0),\delta\mathbf{f}>\\
&=\int_0^\tau\left\langle\frac{\partial\lambda_1(t)}{\partial t}+\left[\frac{\partial F(\mathbf{u})}{\partial\mathbf{u}}\right]^*\lambda_1(t),\delta\mathbf{u}'\right\rangle\mathrm{d}t\\
&+<\mathbf{u}'(\tau)-\lambda_1(\tau),\delta\mathbf{u}'(\tau)>+\\
&+\int_0^\tau\left\langle\frac{\partial\lambda_2(t)}{\partial t}+\lambda_1(t),\delta f\right\rangle\mathrm{d}t+<0\\
&-\lambda_2(\tau),\delta\mathbf{f}>+<\lambda_2(0),\delta\mathbf{f}>,
\end{aligned}
\tag{2.6}
$$

where the sign " [ ]* " denotes an adjoint operator; $\delta\mathbf{u}'(0)=0$ has been taken into consideration. Therefore, by comparing eqs. (2.3) and (2.6), we obtain

$$
\frac{\partial J_1}{\partial\mathbf{f}}=\lambda_2(0). \tag{2.7}
$$

The parameters $\lambda_1(t)$ and $\lambda_2(t)$ in eq. (2.6) satisfy the following relationship:

$$
\begin{cases}
\dfrac{\partial\lambda_1}{\partial t}+\left[\dfrac{\partial F(\mathbf{u})}{\partial\mathbf{u}}\right]^*\lambda_1=0,\\
\dfrac{\partial\lambda_2}{\partial t}+\lambda_1=0,\\
\lambda_1\big|_{t=\tau}=\mathbf{u}'(\tau),\\
\lambda_2\big|_{t=\tau}=0.
\end{cases}
\tag{2.8}
$$

Eqs. (2.8) is the adjoint of eqs. (2.4). By integrating Eqs. (2.8) backward from the prediction time τ to 0, we obtain the gradient $\partial J_1/\partial\mathbf{f}$. With this gradient, the COF can be computed using optimization solvers (the L-BFGS optimization solver is used in this paper).

From eq. (2.6), we know that $\lambda_1(t)$ satisfies the following equations:

$$
\begin{cases}
\dfrac{\partial\lambda_1}{\partial t}+\left[\dfrac{\partial F(\mathbf{u})}{\partial\mathbf{u}}\right]^*\lambda_1=0,\\
\lambda_1\big|_{t=\tau}=u(\tau).
\end{cases}
\tag{2.9}
$$

It is clear that eqs. (2.9) is composed of the adjoint model of the nonlinear model (1.1) with respect to the initial perturbations. It is also obvious that the adjoint model (2.8) associated with model perturbation **f** is established by eqs. (2.9), which are associated with the initial perturbations. Therefore, we do not alter the adjoint model (2.9); rather we only add a line of code for the discretization of the equation $\dfrac{\partial\lambda_2}{\partial t}+\lambda_1=0$ following the code for the adjoint model eqs. (2.9), thereby easily obtaining the adjoint model (2.8).

3 The role of COF in model correction

We use the Lorenz 63 model as an example to analyze the role of constant optimal forcing in model correction. The equations in the Lorenz 63 model are as follows:

$$
\begin{cases}
\dfrac{\mathrm{d}x}{\mathrm{d}t}=-\sigma x+\sigma y,\\
\dfrac{\mathrm{d}y}{\mathrm{d}t}=rx-y-xz,\\
\dfrac{\mathrm{d}z}{\mathrm{d}t}=-bz+xy,
\end{cases}
\tag{3.1}
$$

where σ, r, b are the model parameters with the given values σ=10, r=28 and b=8/3. The Lorenz 63 system is a nonlinear chaotic system and is often used to test the validity of approaches with respect to predictability studies.

In this section, we mainly discuss the effects of model error on the forecast results, and therefore, we assume that the initial field is perfect here. It has been mentioned that model error typically varies with time, and this error is denoted as R. According to the results of D'Andrea and Vautard [15], R can be divided into three parts:

$$
R=\overline{R}+R(\mathbf{u})+R', \tag{3.2}
$$

where $\overline{R}$ is the time-invariant part, i.e., the system error of the model, $R(\mathbf{u})$ is the model error associated with the state vector **u**, and R' is the time-varying part independent of **u** that is usually taken as the uncertainty caused by stochastic process. It is reasonable to believe that the COF method, due to its time-invariant characteristic, can easily reduce the system error, i.e., the time-invariant part of model error. In

this paper, we focus on the role of COF in reducing model errors related to the state vector or/and time-varying stochastic errors.

3.1 Cases of model errors dependent on the state variables

To study the role of the COF in improving forecast capabilities, the forecast results should be compared with observational data. For this section, we choose the well-known Lorenz 63 model to clarify the role of the COF in offsetting model error. The so-called observational data are obtained by running the Lorenz 63 model, and are "ideal". To determine the difference between the model predictions and observations, we use model (3.3) to forecast the "observations" produced by model (3.1).

$$\begin{cases} \dfrac{\mathrm{d}x}{\mathrm{d}t} = -10x + 10y, \\ \dfrac{\mathrm{d}y}{\mathrm{d}t} = 29x - y - xz, \\ \dfrac{\mathrm{d}z}{\mathrm{d}t} = -\dfrac{8}{3}z + xy. \end{cases} \tag{3.3}$$

The difference between the forecast model and the Lorenz 63 model lies in the parameter r, which is equal to 28 in the Lorenz 63 model but has a value of 29 in the forecast model (3.3). In this manner, the uncertainty of r yields the model error. We note that the state variable x is multiplied by r. Therefore, the model error induced by the uncertainty superimposed on r is time-varying during the numerical integration due to the interaction between the parameter error and state variable x. Therefore, the model error induced by the uncertainty of the parameter r corresponds to the model error associated with state variables, i.e., $R(u)$, which is described in eq. (3.2).

Using the fourth-order Rung-Kutta scheme to discretize models (3.1) and (3.3) and integrate them from t=0 to t=5 with initial values x_0=12, y_0=2, z_0=9 and time step dt=0.01, we obtain the "observations" and forecast results of model (3.3), respectively (Figure 1). Note that the initial value of the forecast model is the same as the initial "observations". That is, the initial field of the forecast model is accurate, and we only consider the effect of the model error in the numerical experiment.

Figure 1 shows that the prediction error caused by the model error is relatively small in the forecast time period ($t \leqslant 0.5$) but gradually becomes large after t=0.6. Moreover, the prediction error increases with time, and when $3 \leqslant t \leqslant 3.5$, the forecasted state and the "observed" one are in the opposite phase; thus, the forecast results become useless. Therefore, to obtain more useful forecast results, we must attempt to improve the forecast model. Here, we use the COF method to correct the model and improve the forecast capability of the model.

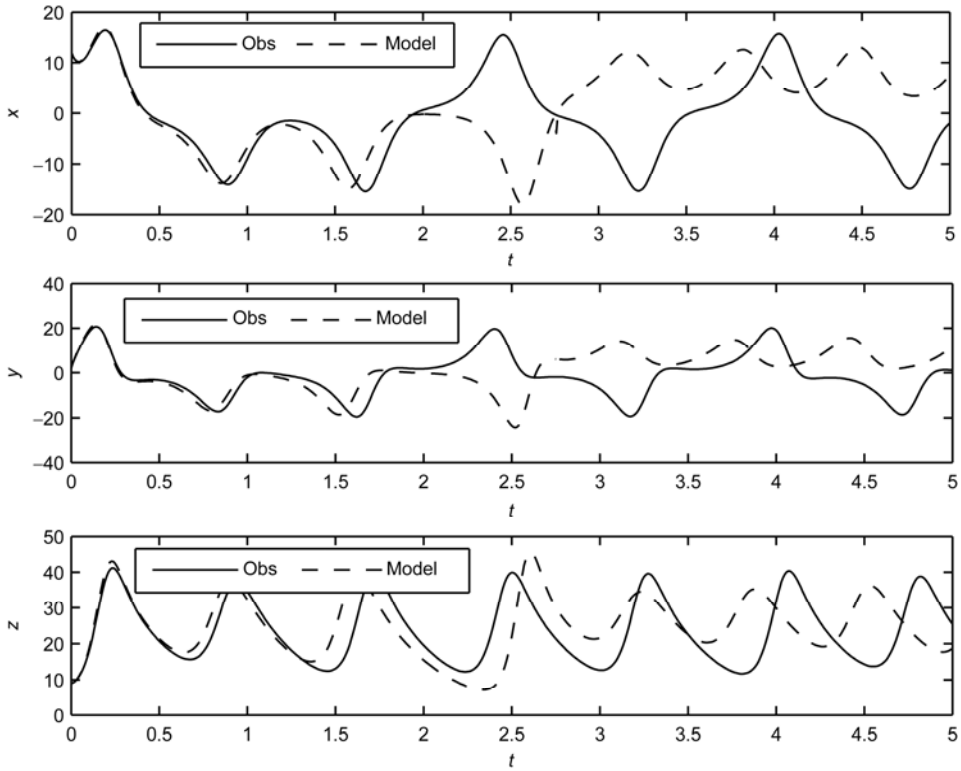

Figure 1 Ideal observations based on Lorenz 63 model (full lines) and forecast results from model (3.3) (dashed lines). *x, y, z* the state variables of Lorenz model.

The objective of the COF method is to add a proper constant forcing to the forecast model (3.3), as shown in Eqs. (3.4). The time interval [0, 1] is chosen as the optimization time interval to compute the COF, and the time intervals [1, 2] are set as the forecast period. Specifically, we use the known "observations" during [0, 1] to obtain the COF and then use the COF to correct the original model to forecast the state vector (x, y, z) during [1, 2].

$$\begin{cases} \dfrac{\mathrm{d}x}{\mathrm{d}t} = -10x + 10y + f_1, \\ \dfrac{\mathrm{d}y}{\mathrm{d}t} = 29x - y - xz + f_2, \\ \dfrac{\mathrm{d}z}{\mathrm{d}t} = -\dfrac{8}{3}z + xy + f_3. \end{cases} \tag{3.4}$$

Taking T=1.0 as the optimization time and using the "observations" during [0, 1], we compute the COF via the L-BFGS method according to Eqs. (1.6) and (1.7) in section 2. This computation shows that the COF of model (3.3) is $\mathbf{f}^{*}=(f_1, f_2, f_3)=(2.8951, 3.0356, 2.9088)^{\mathrm{T}}$. By superimposing it to the eqs. (3.4), we obtain the corrected model. We then use the corrected model to forecast the state variables during [1, 2] (Figure 2). As shown in Figure 2, the results of the corrected model coincide better with the "observations" within both the optimization time window [0, 1] and the forecast time window [1, 2], whereas those of the original forecast model (3.3) deviate significantly from the "observations" over time (Figure 3).

Figure 3 shows the growth of the prediction errors of the original forecast model and the corrected model. Here, the norm used to measure the prediction errors is the L2 norm, i.e., $E_i = \sqrt{x'^2 + y'^2 + z'^2}$ with x', y', z' representing the prediction errors of the variables, where i=1, 2 correspond to the original forecast model (3.3) and the corrected model (3.4), respectively. In other words, E_1 is the prediction error of the original model, and E_2 is the prediction error of the corrected model. It can be shown that over the entire time interval [0, 2], the prediction error of the corrected model is far less than that of the original model, which indicates that the model forecast capability is significantly improved by the COF approach. Therefore, by superimposing the COF calculated from the given "observations" on the forecast model, we obtain much better forecast results within both the optimization and forecast time windows.

3.2 Cases of model errors associated with stochastic process

Climate observations typically include the influence of stochastic processes, whereas forecast models often fail to de-

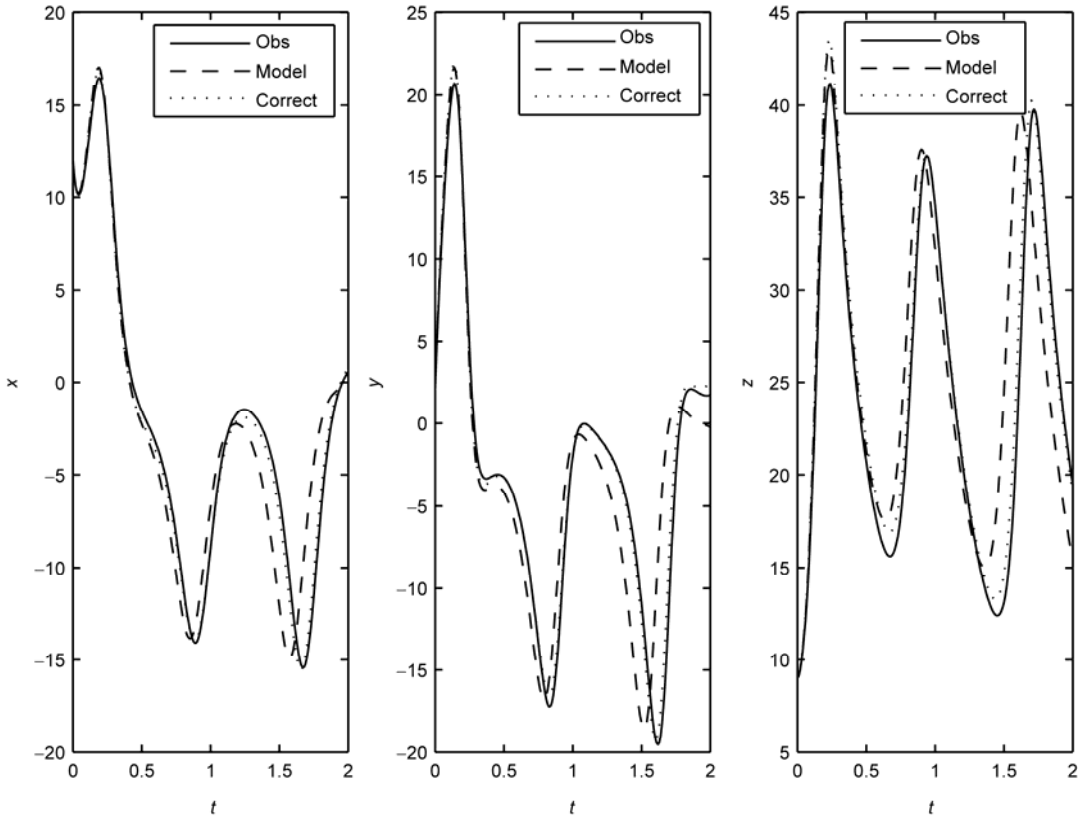

Figure 2 Ideal observations based on Lorenz 63 model (full lines), forecast results from model (3.3) (dashed lines) and from the corrected model (dotted lines). x, y, z the state variables of Lorenz model.

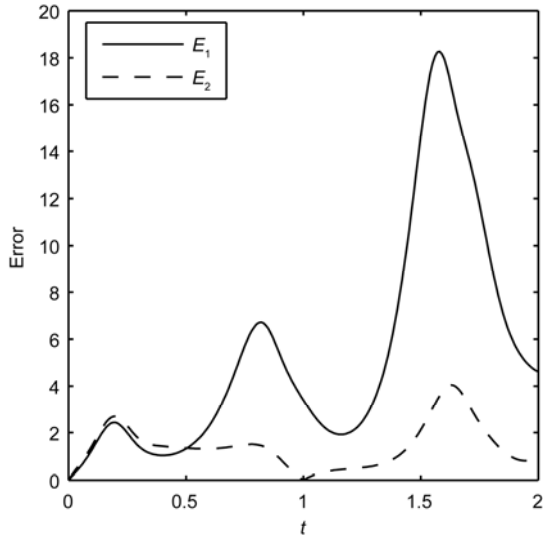

Figure 3 Error growth of model (3.3) (full line) and the corrected model (dashed line).

scribe such processes; as a result, time-dependent random errors are consistently present in the models. This section discusses the influence of the COF in reducing the effect of the random errors. To reflect the observation with random processes, we superimpose random terms onto the Lorenz 63 model and obtain eqs. (3.5) to generate the "observations". Model (3.1) is then used to forecast these "observations":

$$\begin{cases} \dfrac{\mathrm{d}x}{\mathrm{d}t} = -10x + 10y + R_1(t), \\ \dfrac{\mathrm{d}y}{\mathrm{d}t} = 28x - y - xz + R_2(t), \\ \dfrac{\mathrm{d}z}{\mathrm{d}t} = -\dfrac{8}{3}z + xy + R_3(t), \end{cases} \tag{3.5}$$

where $R_1(t)$, $R_2(t)$, $R_3(t)$ represent random noises of a Gaussian distribution with an amplitude given in refs. [2, 4].

Based on eqs. (3.1) and (3.5), it is evident that the model error of the Lorenz 63 model is attributed to the fact that the Lorenz 63 model fails to account for stochastic processes in eqs. (3.5). Clearly, this type of model error is time-varying and corresponds to the random error denoted as R' in eq. (3.2). Therefore, one can ask whether the COF can offset the effect of such random errors on forecast results.

We use a fourth-order Rung-Kutta scheme to discretize eqs. (3.1) and (3.5) and integrate them from initial time 0 to the future time point 5 with initial values x_0=12, y_0=12, z_0=9. Subsequently, the "observations" and the forecast results corresponding to these observations are obtained. Due to the impact of random error, the forecast results generated by the Lorenz 63 model are significantly different from the observations (figures are omitted). Next, we use the COF to revise the model and explore whether it can improve the forecast capability.

The time interval used to compute the COF is taken as [0, 1], and the prediction period is the time interval [1, 2]; i.e., we assume that the "observations" during [0, 1] are known, and we can use these "observations" to compute the COF of the Lorenz 63 model. According to the computation, we obtain the corresponding COF $\mathbf{f}^* = (f_1, f_2, f_3) = (2.8951, 3.0356, 2.9088)^{\mathrm{T}}$. By superimposing this COF onto the Lorenz 63 model, we obtain the corrected model, which is used to forecast the state of the variables during [1, 2] (Figure 4). As shown in Figure 4, the difference between the forecast results generated by the corrected model and the "observations" are extremely small within both the optimization and the forecast time windows; however, there are significant differences between the forecast results generated by the original model and the "observations".

Figure 5 shows the growth of the prediction error of the original and corrected Lorenz 63 models. These results indicate that during the entire time interval [0, 2], the prediction errors of the modified model are approximately zero, whereas those of the original Lorenz 63 model are relatively large. All these results indicate that the forecast capability of the model is improved by adding a COF to the forecast model, and the time-varying random model error is almost eliminated by the COF during the time interval of investigation.

3.3 Cases of the hybrid model errors of parameter and random errors

In sections 3.1 and 3.2, we have shown that when model error is caused only by parameter error associated with the state variables or only by stochastic process, the COF approach is effective at reducing the model error and improving the forecast capability. However, in realistic predictions, these two types of errors often exist simultaneously in a numerical model, and the interaction between these errors also significantly influences the uncertainty of the forecast results. Therefore, we seek to determine the extent to which the COF can offset the model errors caused by these two types of error as well as their interaction.

We use the model (3.5) to generate the "observations", as in section 3.2, and the following model (3.6) is used to forecast the observations:

$$\begin{cases} \dfrac{\mathrm{d}x}{\mathrm{d}t} = -10x + 10y, \\ \dfrac{\mathrm{d}y}{\mathrm{d}t} = 29x - y - xz, \\ \dfrac{\mathrm{d}z}{\mathrm{d}t} = -\dfrac{8}{3}z + xy. \end{cases} \tag{3.6}$$

By comparing model (3.6) with model (3.5), we find that model (3.6) not only fails to describe the model errors

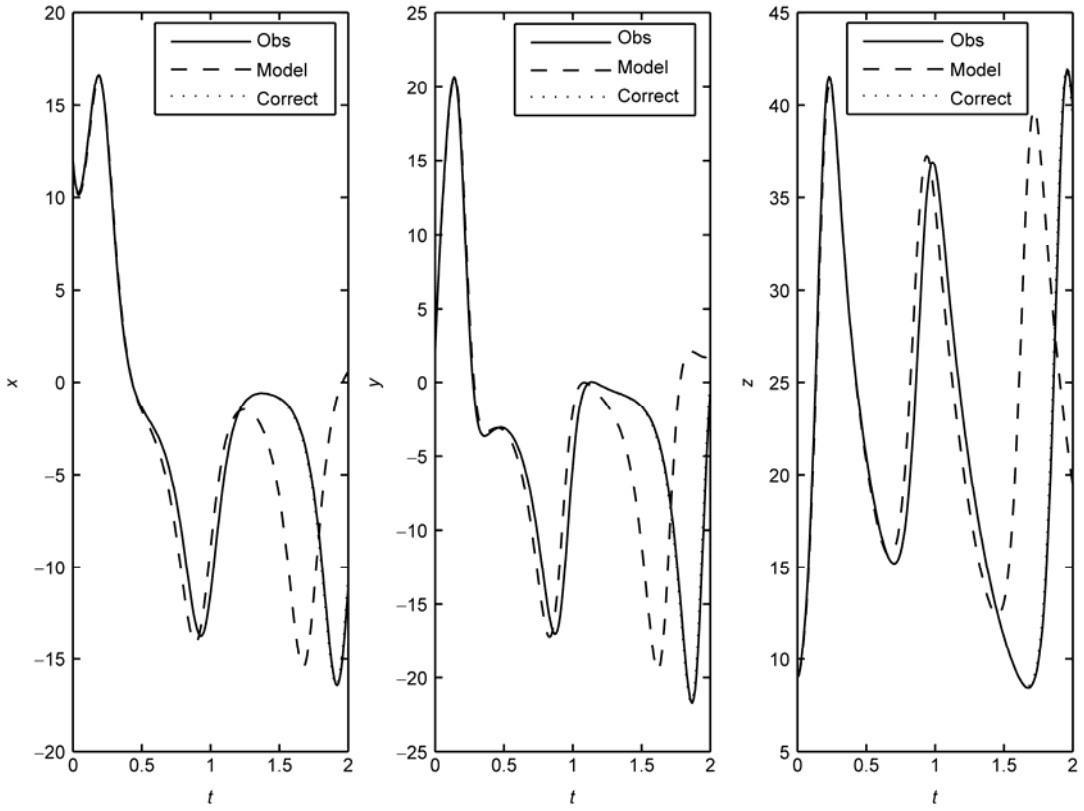

Figure 4 Ideal observations based on model (3.5) (full lines), forecast results from model (3.1) (dashed lines) and from the corrected model (dotted lines). *x, y, z* the state variables of Lorenz model.

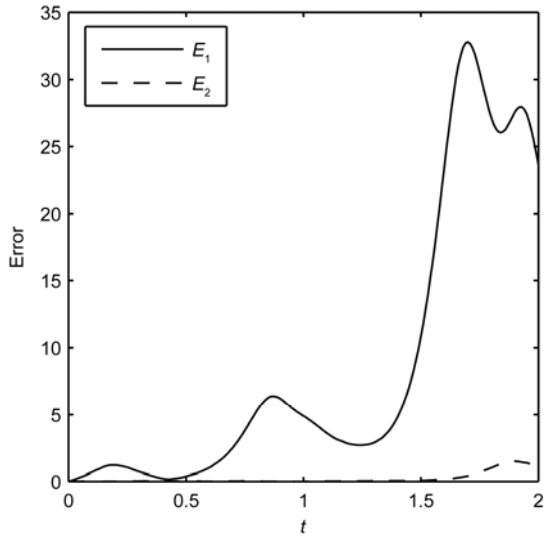

Figure 5 Error growth of model (3.1) (full line)and the corrected model (dashed line).

caused by the random error, but also fails to describe those caused by the parameter errors. The parameter r is equal to 29 in the forecast model (3.6), which is different from that in model (3.5), and this difference induces the model errors.

The COF method is again used to correct the forecast model. As in sections 3.1 and 3.2, the time interval to compute COF is taken as [0, 1], and the time interval of the forecast period is [1, 2]. We then use the "observations" generated by eqs. (3.5) to compute the COF of the forecast model (3.6). The computation shows that the COF of model (3.6) is $\mathbf{f}^* = (f_1, f_2, f_3) = (-1.6297, 7.0150, 5.2176)^{\mathrm{T}}$. By superimposing this model perturbation onto model (3.6), we obtain the corrected model and use it to forecast the state of the physical variables during the time interval [1, 2].

Figure 6 shows the forecast results of state variables (*x, y, z*) obtained by the original forecast model (3.6) and the corrected model. It is clear that the forecast results of the corrected model are in much better agreement with the "observations" than those of the original model (3.6) during [0, 2]. In particular, the prediction error of the corrected model is approximately zero at the optimization time T=1.0. Figure 7 shows the growth of the prediction error of the original model (3.6) and the corrected model. It is readily apparent that, over the entire time interval of [0, 2], the prediction error of the original forecast model (3.6) is significantly reduced by superimposing the COF onto the model. These results indicate that when both parameter error and random error exist in the forecast model, the COF approach remains an effective mechanism to correct the model and improve the forecast capability.

It should be noted that when both parameter error and random error simultaneously exist in the forecast model, the

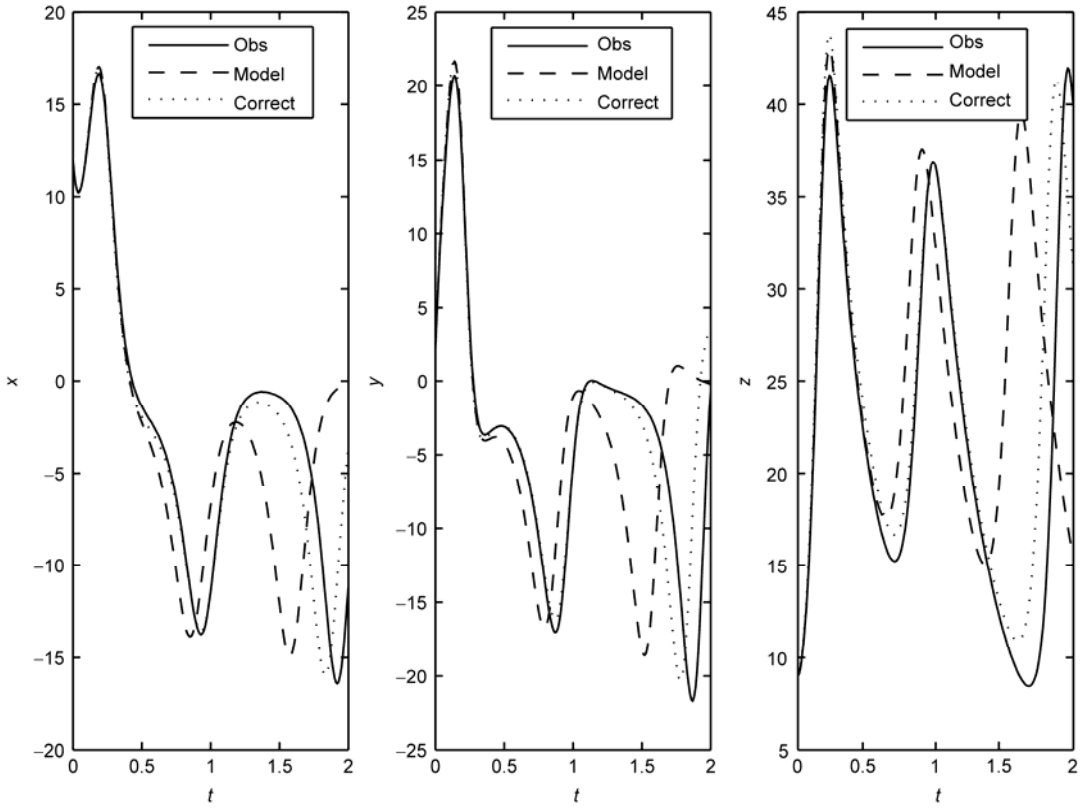

Figure 6 Idea observations based on model (3.5) (full lines), forecast results from model (3.6) (dashed lines) and from the corrected model (dotted lines). *x, y, z* the state variables of Lorenz model.

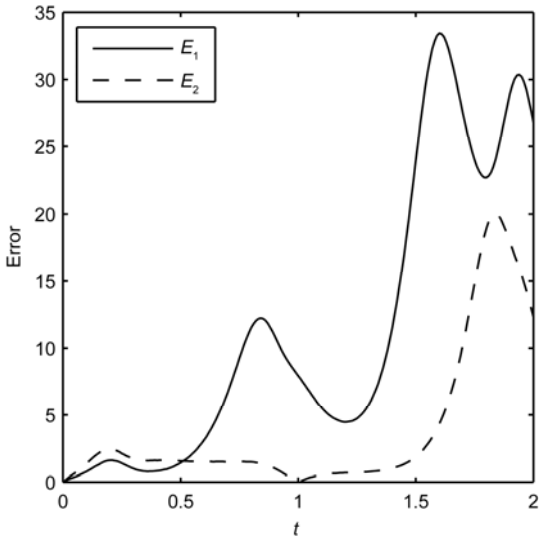

Figure 7 Error growth of model (3.6) (full line) and the corrected model (dashed line).

improvement of the model by the COF is not as evident as in sections 3.1 and 3.2, where only parameter or random errors are considered. In addition, in the numerical experiments, we also find that when only random error is present, the COFs computed at different optimization time intervals do not show large differences from one another, which implies that the COF may be effective for a relatively longer time interval of predictions in reducing the model errors and improving the forecast capability when there is only random error present. However, when both parameter error and random error simultaneously exist in the forecast model, the COFs computed at different optimization time intervals are significantly different. In other words, for the COF of a given time interval, the COF works well in reducing the model error and improving the forecast capability only for a relatively shorter time interval of predictions. This effect reflects the complexity of the interaction of different types of model errors. In addition, the limitation of the COF indicates that it is difficult for one COF to eliminate the multiple sources of model errors. Regardless, we are encouraged by the above results, and the COF approach can be used to offset certain types of model errors and improve the forecast capability to a certain extent. The COF method could be an effective approach that is worth attempting for correcting models and improving forecast capabilities.

4 Discussion and summary

To explore the role of the COF method in correcting forecast models, we derived the gradient formula of the objective function with respect to model perturbation using the adjoint model and then applied this gradient information to compute the COFs of numerical models. Using the Lorenz

63 model as an example, we numerically studied the role of the COF in eliminating different types of model errors. First, we studied the case in which the forecast model only considers parameter errors associated with state variables. The results show that the COF can offset the effect of such model error and thus improve the forecast capability. Second, we explored the case in which the forecast model fails to account for the time-dependent random processes of observational data. In this case, the COF offsets the impact of model error caused by stochastic process and improves the model forecast capability over a longer time than in the former case. Finally, we considered a more realistic case where the model errors are caused by both stochastic process and parameter uncertainties and their interactions. In this case, the COF method is also very effective in reducing model errors. In summary, we demonstrate that although model errors generated by physical process typical vary with time, their effect on forecast results can be effectively reduced by adding a COF to the model. Therefore, the COF method may have a great potential in correcting forecast models and improving the forecast capabilities.

For the model errors caused by parameter errors in section 3.1, we assumed that parameter errors are only derived from parameter r and that the other two parameters are accurate. In numerical experiments, we also explored the situation in which the errors occur in any other parameter or even in multiple parameters. Furthermore, for different magnitudes of errors in various parameters, we also performed numerical experiments and demonstrated similar results. Based on these findings, the COF method is an effective approach for reducing model errors and improving forecast capabilities. For the sake of simplicity, we did not describe the results of every possible scenario in this paper, and only presented the case of errors occurring in the parameter r. In addition, for the parameter errors in the numerical model, we can also directly optimize the parameters to improve the model forecast capability [22]. However, the computation necessary for parameter optimization is more complicated than for the COF, and thus, its application much more difficult in complex forecast models.

In computing the COF in this paper, the purpose is to produce forecast results that are most similar to the "observations" at a given optimization time; therefore, the objective function presented here only measures the magnitude of the prediction error at a given time point. In practical applications, we can define a more reasonable objective function by obtaining forecast results that are most similar to several "observations" at several time points within the optimization time window.

To explain theoretically the role of the COF in improving the model forecast capability, we adopted a conceptual model, i.e., the Lorenz 63 model, to generate "observations" or to act as forecast model. Although this model is simple, the results produced here are encouraging and instructive. In future studies, we will attempt to adopt more realistic forecast models, such as the three-layer baroclinic quasi-geostrophic model, the Zebiak-Cane model, the MM5 model, and the GCM models, to explore the role of COF in correcting models and improving forecast capabilities. It is expected that the COF method will be an effective approach for improving model forecast capabilities in a realistic weather or climate predictions.

This work was jointly sponsored by the National Basic Research Program of China (Grant No. 2012CB955202), the Knowledge Innovation Program of the Chinese Academy of Sciences (Grant No. KZCX2-YW-QN203), and the National Natural Science Foundation of China (Grant No. 41176013).

1 Lorenz E N. Climate predictability. In: The Physical Basis of Climate Modeling. WMO GARP Publ Ser, 1975, 16: 132–136
2 Lorenz E N. Deterministic nonperiodic flow. J Atmos Sci, 1963, 20: 130–141
3 Ott E. Chaos in Dynamical System. Cambridge: Cambridge University Press, 1993. 397
4 Schubert S D, Suarez M. Dynamical predictability in a simple general circulation model: Average error growth. J Atmos Sci, 1989, 46: 353–370
5 Simmons A J, Mureau R, Petroliagis T. Error growth and estimates of predictability from the ECMWF forecasting system. Quart J Roy Meteor Soc, 1995, 121: 1739–1771
6 Leith C E. Numerical simulation of the Earth's atmosphere. In: Alder B, ed. Methods in Computational Physics. New York: Academic Press, 1965. 1–28
7 Charney J G, Fleagle V E, Lally V E, et al. The feasibility of a global observation and analysis experiment. Bull Amer Meteor Soc, 1996, 47: 200–220
8 Lorenz E N. A study of the predictability of a 28 variable atmospheric model. Tellus, 1965, 17: 321–333
9 Lorenz E N. Atmospheric predictability experiments with a large numerical model. Tellus, 1982, 34: 505–513
10 Smagorinsky J. Problems and promises of deterministic extended range forecasting. Bull Amer Meteor Soc, 1969, 50: 286–312
11 Mu M, Duan W S, Wang B. Conditional nonlinear optimal perturbation and its applications. Nonlinear Process Geophys, 2003, 10: 493–501
12 Navon I M, Zou X, Derber J, et al. Variational data assimilation with an adiabatic version of NMC spectral model. Mon Weather Rev, 1992, 120: 1433–1446
13 Evensen G. Sequential data assimilation with a nonlinear quasi-geostrophic model using Monte Carlo methods to prediction error statistic. J Geophys Res, 1994, 99: 10143–10162
14 Ren H L, Chou J F. Study progress in prediction strategy and methodology on numerical model (in Chinese). Adv Ear Sci, 2007, 22: 376–385
15 D'Andrea F, Vautard R. Reducing systematic errors by empirically correcting model errors. Tellus, 2000, 52A: 21–41
16 Roads J O. Predictability in the extended range. J Atoms Sci, 1987, 44: 1228–1251
17 Vannitsem S, Toth Z. Short-term dynamics of model errors. J Atmos Sci, 2002, 59: 2594–2604
18 Qiu C J, Chou J F. A new approach to improve the numerical weather prediction. Sci China Ser B, 1987, 17: 903–908
19 Liu D C, Nocedal J. On the limited memory BFGS method for large scale optimization. Math Program, 1989, 45: 503–528
20 LeDimet F, Talagrand O. Variational algorithms for analysis and assimilation of meteorological observations: Theoretical aspects. Tellus A, 1986, 38: 97–110
21 Zebiak S E, Cane M A. A model El Nino-Southern oscillation. Mon Weather Rev, 1987, 115: 2262–2278
22 Qiu C J, Chou J F. The method of optimizing parameters in numerical prediction model. Sci China Ser B, 1990, 20: 218–224